CrossMark

JM PAPERS

Viscous gravity currents over flat inclined surfaces

Herbert E. Huppert[1], Vitaly A. Kuzkin[2,3] and Svetlana O. Kraeva[2],†

[1]Institute of Theoretical Geophysics, King's College, Cambridge CB2 1ST, UK

[2]Department of Theoretical Mechanics, Peter the Great St Petersburg Polytechnic University, St Petersburg 195251, Russia

[3]Laboratory for Discrete Models in Mechanics, Institute for Problems in Mechanical Engineering RAS, St Petersburg 199178, Russia

Previous analyses of the flow of low-Reynolds-number, viscous gravity currents down inclined planes are investigated further and extended. Particular emphasis is on the motion of the fluid front and tail, which previous analyses treated somewhat cavalierly. We obtain reliable, approximate, analytic solutions in these regions, the accuracies of which are satisfactorily tested against our numerical evaluations. The solutions show that the flow has several time scales determined by the inclination angle, α. At short times, the influence of initial and boundary conditions is important and the flow is governed by both the pressure gradient and the direct action of gravity due to inclination. Later on, the areas where the boundary conditions are important shrink. This fact explains why previous solutions, being inaccurate near the front and the tail, described experimental data with high accuracy. At larger times, of the order of $\alpha^{-5/2}$, the influence of the pressure gradient may be neglected and the fluid profile converges to the square-root shape predicted in previous works. Important extensions of our approach are also outlined.

Key words: gravity currents, general fluid mechanics, lubrication theory

1. Introduction

The study of gravity currents was initiated by von Kármán (1940) in response to being asked by the American military to predict the effects of wind on the propagation of released, relatively heavy, poisonous gas into the atmosphere. Von Kármán developed the famous condition at the front

$$U = Fr\sqrt{g'h}, \tag{1.1}$$

relating the rate of propagation of the current, U, in terms of the height of the current, h, the reduced gravity, g', and the Froude number, Fr, evaluated to be $\sqrt{2}$ under

† Email address for correspondence: kraeva.so96@gmail.com

perfect conditions. Since then, thousands of papers on gravity currents at high Reynolds number have been published (see, for example, Ungarish (2020) for a summary).

The study of the propagation of viscous gravity currents at low Reynolds numbers was initiated by Fay (1969) and Hoult (1972) who used order-of-magnitude analysis to investigate the flow of a thin layer of oil on water. A more complete analysis of the problem, developing the governing equations and presenting their (similarity) form of solution, accurately compared with laboratory experimental measurements, for the propagation above a rigid horizontal surface, was initiated by Huppert (1982), and immediately applied to volcanic domes some ten thousand times larger in horizontal extent on Earth (Huppert *et al.* 1982), some two million times larger on Venus (Head *et al.* 1991) and could no doubt describe the largest volcanic dome in the solar system, Olympus Alba on Mars, which is some 40 million times larger in horizontal extent. Huppert (1982) went on to consider the low-Reynolds-number flow down an incline, again comparing simple theory with laboratory experiments.

Despite the success of these models, each one has potential failings. Von Kármán's model assumes that there is a specific height of the advancing head and that the relevant Froude number is independent of any turbulent motion of the current, which at high Reynolds number there must be. Huppert and Simpson investigated this experimentally and determined that $\sqrt{2}$ (≈ 1.41) should be replaced by 1.19 (Huppert & Simpson 1980). The low-Reynolds-number model assumed that the slope of the flow (i.e. spatial derivative of the fluid thickness) was everywhere small, which is clearly totally incorrect at the (leading) nose. Indeed, it was just this local inaccuracy that induced Huppert (1982) to carry out the confirmatory laboratory experiments (to quieten his collegial critics). The treatment of the front of the flow of the fluid down an incline at low Reynolds number was even more extreme (Huppert 1982); the model front was just cut off and hence had an infinite slope (which is hardly small!). Additionally, in Huppert (1982) it was assumed that the flow is caused by the direct action of the gravitational force only, while the effect of any pressure gradient was neglected. This assumption is doubtful for small inclination angles. The purpose of this paper is to investigate the influence of these approximations.

The next section summarizes previous work, while § 3 develops the full governing equations. Section 4 considers the motion of the head without any further approximations, while § 5 investigates the motion of the tail – without a retaining back wall does it progress upslope or downslope? An approximate analytical solution, satisfying boundary conditions at the front and at the wall, is presented in § 6. The influence of the boundary conditions on the fluid motion is discussed. Numerical verification of hypotheses used in the analytical solutions is carried out in § 7. The influence of the inclination angle on the characteristic time scale of the flow is investigated in § 8. In particular, we show that for any angle (no matter how small) the direct action of gravity due to inclination dominates over the pressure gradient at sufficiently large times. The final section presents a summary and a brief interpretation of our findings.

2. Previous work

In work by Huppert (1982), the flow of a viscous gravity current over a flat surface, inclined at angle α, was considered (see figure 1). The following equation describing the flow was derived:

$$\frac{\partial h}{\partial t} = -3\beta \sin\alpha h^2 \frac{\partial h}{\partial s}, \quad \beta = \rho g/(3\mu), \qquad (2.1a,b)$$
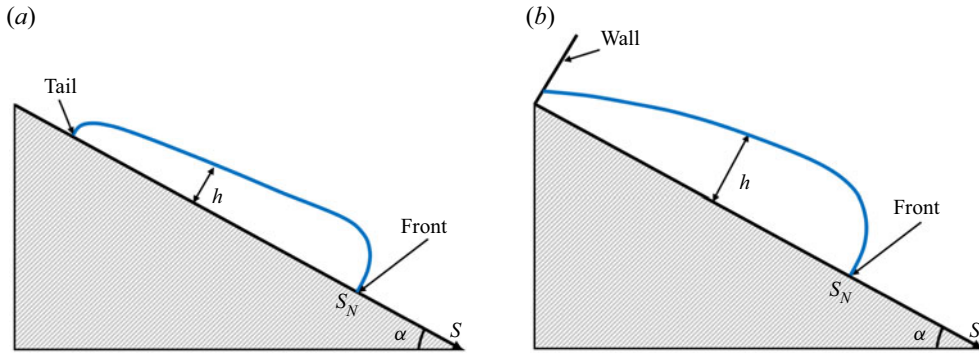
Figure 1. Schematic representation of the gravity current down a flat inclined surface, being unconstrained (*a*) and constrained by a wall (*b*).

where $h(s, t)$ is the fluid thickness at the point s, measured down the plane, ρ is the fluid density, g is the acceleration due to gravity and μ is the dynamic viscosity. The exact, self-similar solution of (2.1*a*,*b*) is

$$
\left.
\begin{aligned}
h(s) &= \sqrt{s/(3t\beta \sin\alpha)}, \quad 0 \le s \le s_N, \\
s_N &= \left(27A^2 \beta t \sin\alpha/4\right)^{1/3}, \quad v_N = 9A^2 \beta \sin\alpha / \left(4s_N^2\right),
\end{aligned}
\right\}
\tag{2.2}
$$

where v_N is the front speed and A is the total fluid area. We note that (2.1*a*,*b*) is approximate. It is based on the assumption that the effect of the hydrostatic pressure gradient is much smaller than the direct action of gravity. This assumption is violated near the front ($s = s_N$) and the tail ($s = 0$) for any α, while it has reasonable accuracy far from these boundaries. Additionally, the solution (2.2) is clearly inaccurate near the front, with a discontinuity in the fluid thickness $h(s, t)$.

Here we examine the influence of these approximations on the accuracy of the solution.

3. Governing equations

In the present section, we derive a general equation, describing the flow of an incompressible fluid over a smooth surface under the action of gravity. The surface is given by the function $r(s)$, where s is a curvilinear coordinate along the surface. A flat inclined surface is a particular case.

The fluid is modelled by a one-dimensional continuum. Each point of the continuum has a velocity v, directed parallel to the tangent to the surface at the point:

$$
v(s, t) = v(s, t)e_\tau(s), \quad e_\tau = \frac{\partial r}{\partial s},
\tag{3.1a,b}
$$

where e_τ is a unit vector, tangent to the surface at point s.

Then the mass balance equation for the fluid has the form

$$
\frac{\partial h}{\partial t} = -\frac{\partial}{\partial s}(hv).
\tag{3.2}
$$

At time t, the fluid occupies the domain $s \in [s_T(t); s_N(t)]$, where $s_T(t)$, $s_N(t)$ are the positions of the fluid tail and the fluid front, respectively. We assume that the motion of

the fluid is quasi-stationary in the sense of slow, low-Reynolds-number motions. If the fluid is bounded by a wall at $s = s_T$ (as considered by Huppert (1982)) then

$$v(s_T) = 0, \quad h(s_N) = 0. \tag{3.3a,b}$$

Otherwise

$$h(s_T) = 0, \quad h(s_N) = 0. \tag{3.4a,b}$$

The total area of the fluid, A, is conserved, i.e.

$$\int_{s_T(t)}^{s_N(t)} h(t)\, \mathrm{d}s = A. \tag{3.5}$$

Here we implicitly assume that h is much less than the local radius of curvature of the surface. If h is not small then the elementary volume is not equal to $h\,\mathrm{d}s$. All further derivations also rely on this assumption.

Neglecting inertial terms in the equation of momentum balance, we obtain

$$\frac{\partial \boldsymbol{F}}{\partial s} + T\boldsymbol{e}_\tau + N\boldsymbol{e}_n + \rho g \boldsymbol{h} = 0, \tag{3.6}$$

where $\boldsymbol{F}$ is the force per unit width acting on the cross-section of the fluid at point s, $\boldsymbol{e}_n$ is the unit vector normal to the surface, T, N are shear and normal stresses acting on the fluid from the surface and $\boldsymbol{g}$ is the gravitational acceleration.

The system of equations (3.2), (3.5), (3.6) is not closed. To close the system, constitutive equations, relating $\boldsymbol{F}$ and T with h and $\boldsymbol{v}$, are required, while N does not enter the resulting equation. We use the following constitutive relations:

$$\left.\begin{aligned} \boldsymbol{F} &= -\rho g h^2 \cos\alpha\, \boldsymbol{e}_\tau/2, \quad T = -3\mu v/h, \\ \sin\alpha &= \boldsymbol{e}_\tau \cdot \boldsymbol{g}/g, \quad \cos\alpha = -\boldsymbol{e}_n \cdot \boldsymbol{g}/g, \end{aligned}\right\} \tag{3.7}$$

where μ is the fluid viscosity and $g = |\boldsymbol{g}|$. According to (3.7), $\boldsymbol{F}$ is proportional to the average hydrostatic pressure multiplied by the fluid thickness, while the expression for T guarantees that (3.9) for $\alpha = 0$ reduces to the result of Huppert (1982).

Substituting (3.7) into (3.6) and multiplying the resulting equation by $\boldsymbol{e}_\tau$, we obtain the expression for the fluid velocity:

$$v = \beta h \left[h \sin\alpha - \frac{1}{2}\frac{\partial}{\partial s}\left(h^2 \cos\alpha \right) \right]. \tag{3.8}$$

Then the mass balance equation (3.2) takes the form

$$\frac{\partial h}{\partial t} = \beta \frac{\partial}{\partial s}\left[\frac{h^2}{2}\frac{\partial}{\partial s}\left(h^2 \cos\alpha \right) - h^3 \sin\alpha \right]. \tag{3.9}$$

Note that in general α may be a function of s. A different form of (3.9) is

$$\frac{\partial h}{\partial t} = \beta \frac{\partial}{\partial s}\left[h^3 \left(\frac{\partial h}{\partial s}\cos\alpha - \left(1 + \frac{h\alpha'}{2}\right)\sin\alpha \right) \right], \quad \alpha' = \frac{\mathrm{d}\alpha}{\mathrm{d}s}. \tag{3.10}$$

Here the first term on the right-hand side describes the effect of the hydrostatic pressure gradient (which decreases with increasing α), while the second term describes the 'direct' influence of the gravitational force.

For the flow along the flat inclined surface ($\alpha' = 0$), (3.9) takes the form

$$\frac{\partial h}{\partial t} = \beta \frac{\partial}{\partial s} \left[h^3 \left(\frac{\partial h}{\partial s} \cos \alpha - \sin \alpha \right) \right]. \tag{3.11}$$

We note that (3.11) reduces to (2.1a,b) only under the assumption $|\partial h/\partial s| \ll |\tan \alpha|$. The influence of this assumption is discussed in § 6.

4. Near-front asymptotics

In this section, we consider the asymptotic behaviour of the solution near the fluid front ($s \to s_N$).

At the front, the function h vanishes, as in (3.4a,b). We then assume that in the vicinity of the front h can be represented as a simple power law of the form

$$h(s) \approx c_1 \, (s_N - s)^\gamma \,. \tag{4.1}$$

Substituting this expression into (3.8), we obtain

$$v \approx \beta \left[c_1^2 \, (s_N - s)^{2\gamma} \sin \alpha + c_1^3 \gamma \cos \alpha \, (s_N - s)^{3\gamma - 1} + \frac{c_1^3}{2} \, (s_N - s)^{3\gamma} \, \alpha' \sin \alpha \right]. \tag{4.2}$$

The front speed v_N is defined as

$$v_N = \dot{s}_N = \lim_{s \to s_N} v. \tag{4.3}$$

We assume that the front velocity is bounded. Then from (4.2) and (4.3), it follows that $\gamma \geq 1/3$. Then two regimes are possible. One possibility is that the front is stationary, $v(s_N) = 0$. This case is considered in § 5. The second possibility is motion of the front with positive velocity. Then

$$v(s_N) > 0, \quad \gamma = 1/3, \quad c_1 = [3v_N/(\beta \cos \alpha_N)]^{1/3}, \quad \alpha_N = \alpha(s_N). \tag{4.4a–d}$$

Note that c_1 depends on the local inclination of the surface. For $\alpha = 0$, formula (4.4a–d) for c_1 coincides with a similar expression obtained for a flat surface by Huppert (1982). We also note that a similar asymptotic approach has been employed by Linkov for simulation of hydraulic fracturing (Linkov 2015).

Note that according to (4.2) the front speed is non-negative. This is a somewhat counterintuitive result. For example, consider an unconstrainted current over a flat inclined surface (see figure 1). In this case the fluid has a front and a tail. It is expected that the fluid will move downslope. From the asymptotics, presented above, it follows that the front indeed moves downslope. In contrast, the tail is either stationary (see e.g. the solution of (2.1a,b), obtained in Huppert (1982)) or it moves up the slope. In the next sections we discuss both front and tail movement.

5. When does the tail not move?

In this section, we address the question of when the tail of fluid on a flat inclined surface is stationary.

Evidently, the tail is stationary if the fluid is bounded by a wall. Then according to (3.3*a*,*b*) and (3.8), the boundary condition at the wall is

$$\frac{\partial h}{\partial s}\bigg|_{s=0} = \tan\alpha. \tag{5.1}$$

The tail may also be stationary in the absence of a constraining wall. If it is so, then the fluid velocity $v(s, t)$, given by (3.8), is positive at least in some vicinity of the tail, i.e.

$$v = \beta h^2 \cos\alpha \left(\tan\alpha - \frac{\partial h}{\partial s}\right) > 0. \tag{5.2}$$

This condition is satisfied only if

$$\frac{\partial h}{\partial s} < \tan\alpha. \tag{5.3}$$

In particular, this condition must be satisfied at $s = s_T$. Then $\partial h/\partial s$ is finite at the tail. Additionally, $h(s_T) = 0$ and therefore near the stationary tail

$$h \approx C(s - s_T)^n, \quad n \geq 1, \quad nC < \tan\alpha. \tag{5.4a–c}$$

Thus the tail is stationary if (5.3) is satisfied. Note that the solution (2.2) violates both conditions (5.1) and (5.3). However, we show below that it has reasonable accuracy at large times, determined in § 8. Additionally, we note that $\partial h/\partial s$ depends on time. Therefore even if the initial conditions satisfy (5.3), it can still be violated later on.

6. An approximate solution

In this section, we derive an approximate solution, describing the flow along a flat inclined surface. As in the real experiments (Huppert 1982), the motion of the tail is excluded by putting a wall at $s = 0$.

We combine the solution (2.2) with the asymptotics (4.1) and the proper boundary condition at the wall (5.1) as

$$h = \begin{cases} 2\tan\alpha\sqrt{s_0(s + s_0)}, & 0 \leq s \leq s_*, \\ [3v_N(s_N - s)/(\beta\cos\alpha)]^{1/3}, & s_* \leq s \leq s_N, \end{cases} \tag{6.1}$$

where $s_0(t)$, $s_*(t)$ are two auxiliary functions. The function s_0 is related to the fluid thickness at the wall as $h(0, t) = 2s_0(t)\tan\alpha$, while s_* is a boundary of the region near the front, where the asymptotics (4.1) is 'important'. We assume that in this region the effect of pressure gradient (proportional to $|\partial h/\partial s|$) dominates over the effect of direct action of gravity (proportional to $\tan\alpha$). Since $|\partial h/\partial s|$ is infinite at the front, such region always exists. As s decreases, $|\partial h/\partial s|$ also decreases, while $\tan\alpha$ is a constant. Therefore at some point the two terms ($|\partial h/\partial s|$ and $\tan\alpha$) become equal. We assume that the asymptotics is

931 A12-6

applicable up to this point, i.e.

$$\left.\frac{\partial h}{\partial s}\right|_{s=s_*} = -\tan\alpha. \tag{6.2}$$

Additionally we require the continuity of the solution at s_*, i.e. $h(s_* - 0) = h(s_* + 0)$. Substituting (6.1) into (6.2) and the continuity condition, we obtain

$$\left.\begin{aligned} s_* &= s_N - \sqrt{v_N/\left(9\beta\sin\alpha\tan^2\alpha\right)}, \\ s_0 &= \left[\sqrt{s_*^2 + v_N/(\beta\sin\alpha\tan^2\alpha)} - s_*\right]/2. \end{aligned}\right\} \tag{6.3}$$

Note that since v_N decreases in time, s_* tends to s_N, while s_0 tends to zero. Therefore intervals at the tail and at the front, where the boundary conditions are important, decrease in time.

Substitution of (6.1) into the global mass balance equation (3.5) yields

$$v_N/(4\beta\sin\alpha\tan\alpha) + 4\tan\alpha s_0^{1/2}[(s_* + s_0)^{3/2} - s_0^{3/2}]/3 = A. \tag{6.4}$$

Equations (6.3) and (6.4) define the dependence of $v_N(s_N)$ in implicit form. This dependence can be treated as the differential equation with respect to the front position. Therefore the approximate solution $h(s, t)$ of (3.11) for a flat inclined surface is given by (6.1), (6.3) and (6.4).

We estimate the range of applicability of the solution (6.1) as follows. Since the solution is only valid for $s_* > 0$, then from (6.3) it follows that

$$s_N^2 > v_N/(9\beta\sin\alpha\tan^2\alpha). \tag{6.5}$$

We assume that for small α, motion of the front may be approximated by the flat surface solution (Huppert 1982), e.g.

$$s_N = \eta_N(\beta A^3 t)^{1/5}, \quad \eta_N \approx 1.411. \tag{6.6}$$

Substituting (6.6) into (6.5), we obtain

$$\beta A^{1/2}t > (45\eta_N\sin\alpha\tan^2\alpha)^{-(5/6)}. \tag{6.7}$$

Then the solution (6.1) is only valid at large times satisfying the condition (6.7). According to (6.7), this time increases with decreasing inclination as $\alpha^{-5/2}$.

To obtain the explicit dependence $v_N(s_N)$, we employ the fact that $s_0 \ll s_*$, because $s_* \approx s_N$, $s_0 = h(0)/(2\tan\alpha)$, $h(0) \ll s_N$. Then (6.3) can be approximately replaced by

$$s_0 \approx v_N/(4s_*\beta\sin\alpha\tan^2\alpha). \tag{6.8}$$

Substituting (6.8) and (6.3) into (6.4), we obtain

$$\left.\begin{aligned} w_N^2/(24\tan^2\alpha) + s_N w_N &= 3A/2, \quad w_N = \left(\frac{v_N}{\beta\sin\alpha}\right)^{1/2}, \\ w_N &= 12\tan\alpha[(s_N^2 + A/(4\tan\alpha))^{1/2} - s_N]. \end{aligned}\right\} \tag{6.9}$$

Since at large times

$$s_N^2 \gg A/(4\tan\alpha), \tag{6.10}$$

the series expansion of (6.9) yields $w_N \approx 3A/(2s_N)$ and

$$v_N \approx 9A^2\beta \sin\alpha/\left(4s_N^2\right). \qquad (6.11)$$

We note that (6.11) coincides with the last formula from (2.2). Using (6.11), we also obtain the approximate expressions for s_0, s_* and $h(0)$:

$$\left. \begin{aligned} s_0/s_N &\approx 9A^2/\left(16s_N^4 \tan^2\alpha\right), \quad s_*/s_N \approx 1 - A/(2s_N^2 \tan\alpha), \\ h(0)/s_N &\approx 9A^2/\left(8s_N^4 \tan\alpha\right). \end{aligned} \right\} \qquad (6.12)$$

These formulae show how s_0 and $h(0)$ tend to zero and s_* tends to s_N with increasing front position s_N. Substitution of (6.12) into (6.1) yields the explicit expression for the fluid profile $h(s/s_N)$.

Thus, at large times (at least satisfying (6.7)), the approximate solution of the 'exact' equation (3.9) coincides with the exact solution of the approximate equation (Huppert 1982). This fact is demonstrated in the following section. The areas where asymptotics (4.1), (4.4a–d) and the boundary condition (5.1) are important decrease in time ($s_* \to s_N$, $s_0 \to 0$). According to (6.12), s_* tends to s_N slower than s_0 tends to zero.

7. Evolution of the fluid profile

In this section, we compare predictions of the approximate analytical solution obtained above with numerical results. The solution predicts that for $\alpha > 0$ at large times the fluid profile converges to the square-root shape (2.2). Using numerical simulations, we show that this is indeed the case.

In numerical simulations, we use a uniform spatial mesh with step Δs. Spatial derivatives in (3.11) are approximated by finite differences. The resulting system of difference equations is solved numerically using the implicit numerical scheme described in Appendix A. Initially, the fluid occupies a square of width $A^{1/2}$. The following values of dimensionless parameters were used: $\alpha = \pi/12$, $\Delta s/A^{1/2} = 0.003$, $\beta \Delta t A^{1/2} = 0.033$. Evolution of the fluid profile $h(s, t)$ is shown in figure 2(a). As predicted by the analytical solution (2.2), the area where asymptotics is important shrinks in time. The profile rapidly converges to the square-root-like shape, predicted by both solutions (2.2) and (6.1). The time required for the convergence as a function of the inclination angle α is estimated in the following section. At large times, the solution near the front becomes very steep (see figure 2b). This fact justifies approximation of the solution by the discontinuous function (2.2).

8. What is a 'small' inclination angle?

Solutions for flat (Huppert 1982) and inclined (Huppert 1982) surfaces are significantly different. For example, in the flat case, the fluid front propagates as $t^{1/5}$, while in the inclined case it propagates as $t^{1/3}$ (see formula (2.2)). Thus two questions arise. Which solution should be used if the inclination angle is small? And what angle can be regarded as small? In this section, we answer these questions by analytical and numerical analysis of (3.11).

Equation (3.11) contains two 'forces' driving the flow, namely the pressure gradient proportional to $\partial h/\partial s$ and the direct action of gravity proportional to $\sin\alpha \sim \alpha$. If $|\partial h/\partial s| \gg \alpha$ then the flat surface solution will be valid. However, at large times $\partial h/\partial s$
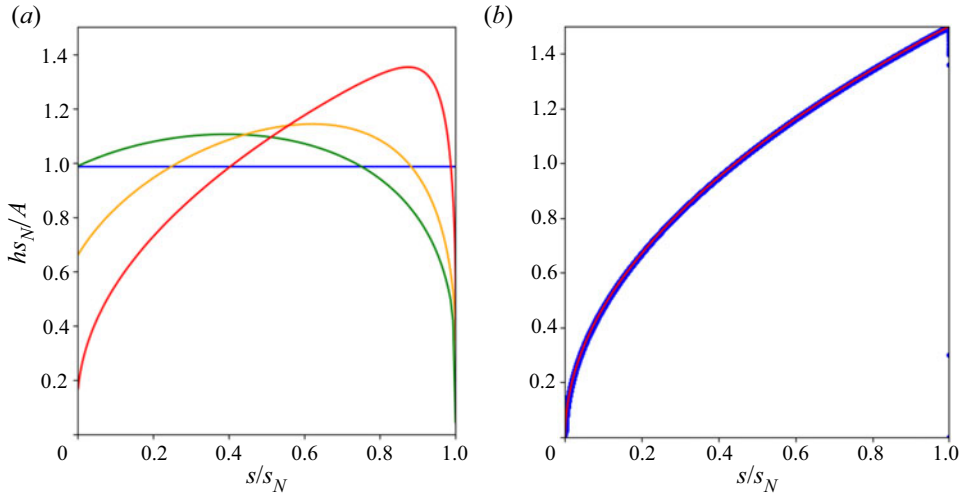
Figure 2. (*a*) Normalized fluid profile hs_N/A at short times $\beta t A^{1/2} = 0$ (blue line), 1.58 (green line), 15.8 (yellow line) and 316.2 (red line). (*b*) Normalized fluid profile hs_N/A at large times ($\beta t A^{1/2} = 1.9 \times 10^7$). Numerical solution (blue dots) and analytical solution (2.2) (red line) are shown.

tends to zero. Therefore the flat surface solution will be valid for a certain time scale only. At larger times, the term proportional to α will always dominate. Therefore at large times the inclined surface solution (2.2) is more relevant.

We estimate the time scale at which the inclination starts to dominate over the pressure gradient as follows. We find a time such that $\partial h/\partial s$ and α are of the same order. Assuming that at short times the flat surface solution is valid, we obtain that the fluid front propagates as $t^{1/5}$ (see Huppert 1982). Since the total fluid volume is conserved, the fluid thickness decreases as $t^{-(1/5)}$. Then the following estimate is valid:

$$\frac{\partial h}{\partial s} \sim (\beta A^{1/2} t)^{-(2/5)}. \tag{8.1}$$

Assuming $\partial h/\partial s \sim \alpha$, we obtain

$$\beta A^{1/2} t \sim \alpha^{-(5/2)}. \tag{8.2}$$

Note that a similar power law follows from (6.7). Formula (8.2) shows that the characteristic time scale at which the inclination becomes dominant rapidly increases with decreasing α and tends to infinity as α tends to zero.

Our numerical simulations, carried out at different inclination angles α from $2°$ to $30°$, support this conclusion. The simulations show that for all angles the fluid profile converges to the square-root shape. The time, t_c, required for convergence strongly depends on α. To estimate this dependence we perform simulations with different values of α and compute the difference ε between the numerical solution h_n and the analytical solution h_a, defined by (2.2). The difference is defined by

$$\varepsilon(t) = \frac{1}{N(t)} \sum_{i=1}^{N(t)} |h_n^i - h_a|/h_n^i, \tag{8.3}$$

where h_n^i is the fluid thickness at node i and $N(t)$ is the total number of nodes occupied by the fluid at time t.
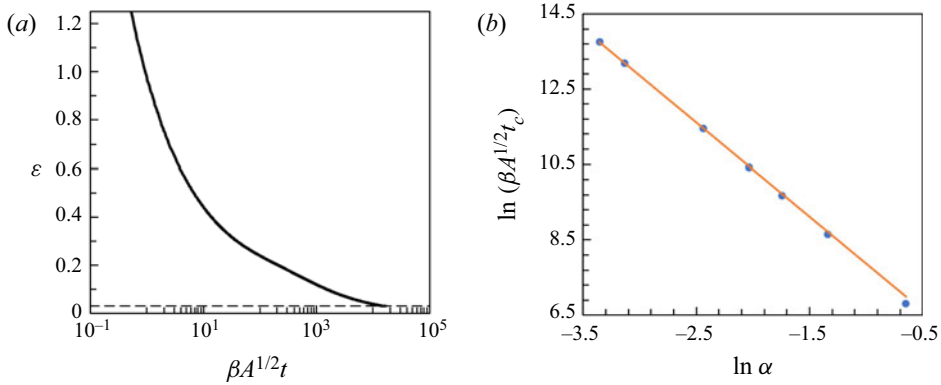
Figure 3. (*a*) Relative deviation, ε, of the numerical solution from the square-root solution (2.2) for $\alpha = \pi/18$. Dashed line corresponds to $\varepsilon = 0.03$. (*b*) Time required for convergence of the fluid profile to the square-root shape as a function of the inclination angle α. Numerical results (dots) and fitting line (8.4) are shown.

Numerical simulations show that ε decreases in time (see figure 3*a*). We define the time required for convergence, t_c, as the minimal time satisfying $\varepsilon(t) \leq 0.03$ (see dashed line in figure 3*a*). Using (8.2), we fit the dependence of t_c on α by the power law

$$\beta A^{1/2} t_c = C\alpha^{-(5/2)}, \tag{8.4}$$

where $C \approx 214$. Figure 3(*b*) shows that formula (8.4) approximates the numerical results with very good accuracy for all considered inclination angles.

Thus at large times the effect of inclination (direct action of gravity) dominates over the pressure gradient and the fluid profile converges to the square-root shape, predicted by (2.2). The time required for convergence tends to infinity with decreasing inclination angle as $\alpha^{-5/2}$.

9. Conclusions

We have brought up to date the understanding of the expected motions of both the head and tail of a low-Reynolds-number viscous gravity current propagating down an inclined plane at a fixed angle. Our main quantitative analytical results, presented mainly in § 6, are confirmed by numerical evaluation in §§ 7 and 8. A short summary of our findings is that the problem has several different time scales. At short times the influence of initial and boundary conditions is important and the flow is governed by both pressure gradient and the direct action of gravity. Later on, the areas where the boundary conditions are important shrink. This fact explains why solution (2.2), being inaccurate near the front and the tail, described the experimental data with high accuracy. At larger times, of the order of $\alpha^{-5/2}$, the influence of the pressure gradient may be neglected and the fluid profile converges to the square-root shape (2.2). We note that the vanishing importance of the boundary conditions, confirmed by numerical simulations, follows from the approximate solution (6.1), which was guessed rather than derived. Therefore more rigorous proof of this phenomenon would be an interesting extension of the present work.

Our analysis is a first step in the investigation of the form of motion of a low-Reynolds-number, viscous gravity current over an uneven, bumpy surface, where both pressure gradient and gravity play an essential role. In these circumstances the flow may even cease, constrained by the boundaries. We have already initiated the investigation of such situations and plan to submit the work for publication in the near future.

Author ORCIDs.

Herbert E. Huppert https://orcid.org/0000-0002-0185-0598;

Vitaly A. Kuzkin https://orcid.org/0000-0003-0484-0106;

Svetlana O. Kraeva https://orcid.org/0000-0002-6390-2410.

Appendix A

For numerical analysis of the fluid flow, we rewrite (3.11) in dimensionless form as

$$
\begin{aligned}
\frac{\partial \tilde{h}}{\partial \tilde{t}} &= \frac{\partial}{\partial \tilde{s}} \left[\tilde{h}^3 \left(\frac{\partial \tilde{h}}{\partial \tilde{s}} \cos\alpha - \sin\alpha \right) \right], \\
\tilde{s} &= s/A^{1/2}, \quad \tilde{h} = h/A^{1/2}, \quad \tilde{t} = \beta t A^{1/2},
\end{aligned} \tag{A1}
$$

where A is the fluid area.

By using the implicit scheme, (A1) can be written in a discretized form as

$$
\begin{aligned}
\frac{h_i^{k+1} - h_i^k}{\Delta t} = \frac{1}{\Delta s^2} &\left\{ \left(h_{i-1/2}^k \right)^3 \left[\left(h_{i-1}^{k+1} - h_i^{k+1} \right) \cos\alpha - \sin\alpha \right] \right. \\
&\left. - \left(h_{i+1/2}^k \right)^3 \left[\left(h_i^{k+1} - h_{i+1}^{k+1} \right) \cos\alpha - \sin\alpha \right] \right\},
\end{aligned} \tag{A2}
$$

where $h_{i-1/2}^k = (h_{i-1}^k + h_i^k)/2$ and $h_{i+1/2}^k = (h_i^k + h_{i+1}^k)/2$. The tridiagonal matrix algorithm is used to solve this equation at each time step.

In order to trace the front position $s_N(t)$, the following equations were used:

$$
s_N^{k+1} = s_N^k + v_N^{k+1} \Delta t, \quad v_N^{k+1} = \frac{\left(h_{n-1}^{k+1} \right)^3 \cos\alpha}{3(s_N^k - s_{n-1})}, \tag{A3a,b}
$$

where n is the front node, from which we assume there is no flux to the next $n + 1$ node. As fluid propagates further to the point s_{n+1} we change our front node to $n + 1$.

For physical reasons, the numerical scheme must be positivity conserving to guarantee that h is always positive. We do not have a rigorous proof of positivity for the numerical scheme (A2). However, the condition $h > 0$ has been monitored in all simulations. It has never been violated.

REFERENCES

FAY, J.A. 1969 The spread of oil slicks on a calm sea. In *Oil on the Sea* (ed. D.P. Hoult), pp. 53–63. Plenum.

HEAD, J.W., CAMPBELL, D.B., ELACHI, C., GUEST, J.E., MCKENZIE, D.P., SAUNDERS, R.S., SCHABER, G.G. & SCHUBERT, G. 1991 Venus volcanism: initial analysis from Magellan data. *Science* **252**, 276–288.

HOULT, D.P. 1972 Oil spreading on the sea. *Annu. Rev. Fluid Mech.* **4**, 341–368.

HUPPERT, H.E. 1982 Flow and instability of a viscous current down a slope. *Nature* **300** (5891), 427–429.

HUPPERT, H.E. 1982 The propagation of two-dimensional and axisymmetric viscous gravity currents over a rigid horizontal surface. *J. Fluid Mech.* **121**, 43–58.

HUPPERT, H.E., SHEPHERD, J.B., SIGURDSSON, H. & SPARKS, R.S.J. 1982 On lava dome growth, with application to the 1979 lava extrusion of the soufriere of St. Vincent. *J. Volcanol. Geotherm. Res.* **14**, 199–222.

HUPPERT, H.E. & SIMPSON, J.E. 1980 The slumping of gravity currents. *J. Fluid Mech.* **99**, 785–799.

VON KARMAN, T. 1940 The engineer grapples with nonlinear problems. *Bull. Am. Math. Soc.* **46**, 615–683.

LINKOV, A.M. 2015 The particle velocity, speed equation and universal asymptotics for the efficient modelling of hydraulic fractures. *J. Appl. Math. Mech.* **79** (1), 54–63.

UNGARISH, M. 2020 *Gravity Currents and Intrusions: Analysis and Predictions*. World Scientific.